Flight Dynamics Investigation of Compound Helicopter Configurations

Kevin M. Ferguson*, Douglas G. Thomson†,
University of Glasgow, Glasgow, United Kingdom, G12 8QQ

Compounding has often been proposed as a method to increase the maximum speed of the helicopter. There are two common types of compounding known as wing and thrust compounding. Wing compounding offloads the rotor at high speeds delaying the onset of retreating blade stall, hence increasing the maximum achievable speed, whereas with thrust compounding, axial thrust provides additional propulsive force. There has been a resurgence of interest in the configuration due to the emergence of new requirements for speeds greater than those of conventional helicopters. The aim of this paper is to investigate the dynamic stability characteristics of compound helicopters and compare the results with a conventional helicopter. The paper discusses the modeling of two compound helicopters, which are named the coaxial compound and hybrid compound helicopters. Their respective trim results are contrasted with a conventional helicopter model. Furthermore, using a numerical differentiation technique, the dynamic stability of each configuration is assessed. The results show that the frequency of the coaxial compound helicopter's dutch roll mode is less than that of the conventional helicopter and there is also greater roll damping. Concerning the hybrid compound helicopter, there is greater roll damping and the phugoid mode stabilizes at high speeds.

Nomenclature

$\mathbf{f}$	forcing vector function
g	acceleration due to gravity (m/s^2)
u, v, w	translational velocities (m/s)
$\mathbf{u}$	control vector
v_0	uniform induced velocity component (m/s)
$\mathbf{x}$	state vector
$\mathbf{x}_{\text{prop}}$	position of the propeller hub (m)
$\mathbf{A}, \mathbf{B}$	system and control matrices
C_q, C_t	torque and thrust coefficient
C_{t_u}, C_{t_l}	upper and lower rotor thrust coefficient
I_β	flap moment of inertia (kgm^2)
K_β	centre-spring rotor stiffness (Nm/rad)
L_p	roll damping derivative (1/s)
L_v	dihedral derivative (rad/ms)
M_q	pitching damping derivative (1/s)
M_u	speed stability derivative (1/s)
N_b	number of rotor blades
N_p	yawing moment due to roll rate (1/s)
P	coaxial rotor power (HP)
R, R_{prop}	radius of the main rotor and propeller blades (m)
U_e	forward speed at trim (m/s)
U_p	normal velocity of a rotor blade element (m/s)
U_t	tangential velocity of a rotor blade element (m/s)
X_{port}, X_{star}	port and starboard propeller thrust (N)
X_u	drag damping derivative (1/s)
α_w	angle of attack of a wing element (rad)
γ	Lock number
γ_s	rotor shaft tilt (rad)
λ_l,λ_u	non-dimensional lower and upper rotor inflow
μ	non-dimensional advance ratio
μ_z	non-dimensional normal velocity of the rotor hub
ω	frequency (rad/s)
ω_{dr}	dutch roll mode frequency (rad/s)
Ω , Ω_{prop}	main rotor and propeller rotational speed (rad/s)
ϕ, θ	Euler angles (rad)
ϕ_i	rotor inflow angle (rad)
σ,σ_{prop}	rotor and propeller solidity
θ_{fixed}	fixed wing pitch incidence (rad)
θ_{diff}	differential collective (rad)
θ_l, θ_u	lower and upper rotor collective pitch (rad)
$\bar{\theta}_{\text{prop}}$	mean collective setting of the two propellers (rad)
θ_{tw}	gradient of linear twist (rad)
θ_0	main rotor collective pitch angle (rad)
$\bar{\theta}_0$	mean upper and lower rotor collective pitch (rad)
$\theta_{1\text{s}}$,$\theta_{1\text{c}}$	longitudinal and lateral cyclic pitch (rad)

I. Introduction

The compound helicopter has experienced a resurgence of interest recently due to its ability to obtain speeds that significantly surpass the conventional helicopter. This increase in speed makes the compound helicopter suitable for various roles and missions such as troop insertion, search and rescue, ship replenishment as well as short haul flights in the civil market. The compounding of a helicopter is not a new idea but the development of a compound helicopter has proven elusive for the rotorcraft community due to a combination of technical problems and economical issues [1]. The rotorcraft community is again exploring the compound helicopter design, with Sikorsky and Eurocopter both testing their prototypes. The Sikorsky X2 is a coaxial design with thrust compounding whereas the Eurocopter X^3 is a conventional single rotor machine with both thrust and wing compounding.

The maximum speed of a conventional helicopter is restricted due to aerodynamic limitations, installed engine power and airframe drag [2]. The problems associated with installed engine power and airframe drag can be minimized through careful design, but the main factor limiting the maximum speed of the helicopter is retreating blade stall. The compound helicopter is designed to delay the flight speed at which the condition of retreating blade stall occurs thereby increasing the maximum operating speed of the vehicle. Both the Sikorsky X2 and the Eurocopter X^3 have different methods to avoid retreating blade stall until higher speeds. The X2, with its coaxial rotor, uses the ABC (Advancing Blade Concept) rotor system to offload the retreating side of the disc at high speeds and therefore avoid blade stalling. This concept was originally developed in the 1960s but the aircraft never entered production [3]. Recently, the ABC rotor system has been revisited and the design improved upon with the use of advanced airfoil sections and active vibration control [4, 5]. Due to these improvements as well as the pusher propeller providing an extra component of axial thrust, the Sikorsky X2 is able to reach speeds of 250 knots [6].

In contrast, the wings of the Eurocopter X^3 offload the rotor at high speeds and the propellers provide the propulsive force to overcome the fuselage drag. Recent publications have reported that the Eurocopter X^3 is able to reach a maximum speed of 232 knots. It is therefore evident that these helicopters are capable of greater speeds than their conventional counterparts.

As mentioned previously, the compounding of the helicopter is not

*Currently a PhD Student, Aerospace Sciences Division, School of Engineering, email: k.ferguson.1@research.gla.ac.uk

†Senior Lecturer, Aerospace Sciences Division, School of Engineering, email: Douglas.Thomson@glasgow.ac.uk

a novel idea. There have been various flight test programs that have investigated the compound helicopter configuration [7–10]. Although these programs never led to a production vehicle, they did provide some insight into the problems that designers may face with the development of a compound helicopter. One issue is the inherent control redundancy that results from compounding the conventional configuration. The compounding results in an additional control relative to a conventional helicopter and therefore there is an issue on how to integrate this control into the vehicle. The Rotor Systems Research Aircraft (RSRA) conducted a series of flight tests which featured a fixed setting of collective pitch [7]. This set-up offers a reduction in terms of pilot workload but does not fully exploit the additional control offered by compounding. A successful compound helicopter would require a control system that exploits the additional control to enhance the performance benefits that compounding offers without significantly increasing pilot workload. Another issue that arose from the flight test programs of the XH-51A helicopter [8] was the tendency of the rotor to overspeed. During high speed maneuvers the load factor of the main rotor increased quicker than that of the wing thus resulting in rotor overspeed. The AFCS would have to reduce the collective pitch setting of the main rotor in high speed maneuvers, thereby avoiding rotor overspeed. The Lockheed Cheyenne, another notable compound helicopter, encountered problems with its gyro design which led to a fatal crash [9]. The combination of this crash, other problems with the design and political issues ended the Cheyenne program despite the vehicle exhibiting excellent performance. It is clear that the compounding of a helicopter presents some problems, all of which will have to be overcome, or at least ameliorated, but the advantages, in terms of increasing the maximum speed of the helicopter, are clear.

More recently, Orchard et al. focused on the design of the compound helicopter [11]. Their study investigated the various design aspects of a compound helicopter such as the wing, rotor and propulsor design. The study suggests that a medium size wing should be used to provide a compromise between the beneficial effect of offloading the rotor at high speeds and the adverse effect of creating aerodynamic download at low speeds. To optimize the compound design, most authors agree that a wing must be supplemented with auxiliary propulsion [12–15]. The reason for this is that a wing-only compound helicopter tends to have a more pitch down attitude, relative to a baseline helicopter [12]. In forward flight, the wing offloads the main rotor and therefore reduces the rotor thrust. The rotor thrust is still required to overcome the fuselage drag as well as the additional drag of the wing, hence to trim the helicopter the smaller rotor thrust vector must be tilted more forward to provide the propulsive force. As a result, the pitch of the helicopter tends to be more nose down than that of the baseline configuration which reduces the angle of attack of the wing and therefore its lifting capability. However, if auxiliary propulsion is introduced the pitch attitude can be controlled, therefore fully exploiting the lifting capability of the wing. An alternative approach to increasing the maximum speed of the helicopter is the 1950's Gyrodyne concept that was recently revisited by Houston [16]. The Gyrodyne concept employs a propulsor mounted onto a side of the fuselage to replace the tail rotor and therefore fulfill the dual role of providing axial thrust and the anti-torque moment. Houston used the Puma SA330 helicopter in his study and showed that this Gyrodyne set-up increased the maximum speed of the helicopter by 50 knots.

It is clear that there is no shortage of literature concerning the compound configuration, all of which confirms the potential advantages of the vehicle. The next logical question relates to the dynamic stability of this aircraft class, and its affect on flying qualities and control. The main aim of this paper is to assess the dynamic stability of compound helicopters and compare their stability to a conventional helicopter. The strategy for the current work is to use an established mathematical model of a conventional helicopter (in this case the AgustaWestland Lynx), then convert this model to represent compound configurations. The Lynx was chosen as a well established data set [17] and model was available [18]. The compound configurations that are examined in the paper are similar to the Sikorsky X2 and Eurocopter X^3. The first compound model is referred to as the Coaxial Compound Helicopter (CCH) Model which features a coaxial rotor and a pusher propeller as seen in Figure 1a. The second model is known as the Hybrid Compound Helicopter (HCH) model which features a wing and two propellers, as seen in Figure 1b. These two compound models are changed as little as possible, relative to the baseline model, to allow for a fair and direct comparison between the results of the compound configurations and the baseline (BL) model. Therefore, unless stated, the design features of the compound helicopter models are identical to that of the conventional Lynx helicopter. The result is two rather unusual looking vehicles, Figures 1a and 1b, however it should be stressed that this is not a design exercise, and so to ensure that the effects of compounding are isolated from other factors, the basic vehicle shape and size is maintained.

II. Methodology

The compound helicopter models are developed using the Helicopter Generic Simulation (HGS) model [17, 18]. The HGS model is a conventional disc-type rotorcraft model, as described by Padfield [17], and has found extensive use in studies of helicopter flight dynamics. The HGS model is generic in structure, with only the helicopter's parameters required to model the vehicle. The main rotor model, within the HGS package, ignores the pitching and lagging degrees of freedom therefore assuming that the flap dynamics have the most influence in terms of the helicopter's flight dynamic characteristics. The flap dynamics are assumed to be quasi-steady, a common assumption in main rotor modeling, therefore permitting a multi-blade representation of the main rotor. The rotor model neglects the rotor periodicity by assuming that only the steady components of the periodic forces and moments generated by the main rotor influence the helicopter's body dynamics. The main rotor is assumed to be centrally hinged with stiffness in flap with the main rotor chord assumed to be constant. Furthermore, the model also features dynamic inflow, and rotorspeed governor model. One important assumption, within the rotor model, is that the aerodynamics are linear, so that the lift is a linear function of the local blade angle of attack whereas the drag is modeled by a simple polynomial. Due to this assumption, non-linear aerodynamics such as retreating blade stall and compressibility are not modeled. To model the non-linear aerodynamics and rotor periodicity requires an "individual blade model", such as the main rotor model developed by Rutherford and Thomson [19] and further improved upon by Doyle and Thomson [20]. Regarding the modeling of the other subsystems of the rotorcraft, the forces and moments of the tailplane, fuselage and fin calculated using a series of look-up tables derived from experimental data.

One question that naturally arises is the validity of these models and if the results from these rotorcraft models would replicate the real aircraft. In terms of the conventional helicopter, inverse simulation results have shown good correlation for a range of maneuvers [21] giving confidence to the worth of the results produced by the HGS model. The limitations of this type of model are well understood [17] and include the inability to accurately capture off-axis effects and low fidelity at the edges of the flight envelope where, for example, aerodynamic are highly non-linear. In relation to the compound helicopter models, a strict validation based on the comparison of flight test with simulation results is not possible as these are hypothetical vehicles. However, it is believed that the mathematical models would correctly represent the basic physics of the compound helicopters. It should be also be noted that the compound models can be trimmed for flight speeds that exceed 200 knots. However, in this study, 200 knots it is assumed to be the helicopter's boundary for two reasons. Firstly, at high speeds it can be expected that compressibility effects become significant increasing the rotor torque and secondly, at high speeds a large portion of the retreating side of disc would be operating in reverse flow. The current rotorcraft model does not model these non-linear aerodynamic phenomenon and it is reasonable to expect that these effects could produce unrealistic results in flight speeds in excess of 200 knots. The HGS package was developed to simulate a conventional helicopter. Therefore models of a coaxial rotor, propeller and wing are missing from the package. The following section provides an overview of these models.

A. Coaxial Rotor Model

The coaxial rotor is modeled by using two multi-blade rotor models spaced vertically apart. The upper rotor rotates in an anti-clockwise direction (when viewed from above) whereas the lower rotor rotates in a

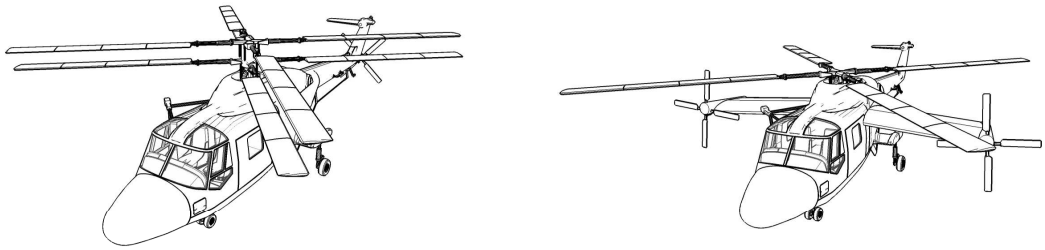

a) Coaxial Compound Helicopter Sketch **b) Hybrid Compound Helicopter Sketch**

Figure 1. Sketches of the two Compound Helicopter Models

clockwise direction. In terms of a conventional single rotor, the Pitt and Peters dynamic inflow model [22] is the most commonly used in helicopter flight dynamics. An equivalent model representing the inflow through a coaxial rotor is not available within literature and the development of such a model is beyond the scope of the current work. With the growth of interest in coaxial rotors, partly due to the development of the Sikorsky X2, clearly there is need for such a model and an appropriate test data for validation. For the time being, a simple steady momentum theory approach, used in simple conventional rotor models, is adapted to represent the inflow of a coaxial configuration. This version assumes that the induced velocity changes instantaneously across the rotor disc, therefore not faithfully modeling the dynamic lag of the induced velocity [23]. In terms of steady coaxial inflow models, various have been created with Leishman et al. [24, 25] developing a coaxial inflow model by slightly adapting the classical blade element momentum approach. The results show very good agreement with experiment in hover and in axial flight. Kim and Brown used another approach, using the vorticity transport model (VTM) to estimate the performance of a coaxial rotor [26, 27]. The coaxial rotor inflow model used here is a similar inflow model to that of Leishman's et al., with a few adaptations. The first assumption made in the development of the coaxial inflow model is that the inflow of the lower rotor does not affect the upper rotor's ability to generate thrust. The second assumption is that the rotors are sufficiently close together that the wake from the upper rotor does not contract radially inward and does not fully develop. This assumption can be justified as it assumed that the rotor is similar to that of the ABC rotor, featuring very stiff blades with a small separation distance between the rotors. Hence the relationship between the rotor thrust and the induced velocity of the upper rotor is

$$C_{t_u} = \lambda_u \sqrt{\mu^2 + (\mu_z - \lambda_u)^2} \tag{1}$$

The lower rotor's inflow consists of a combination of its own induced velocity and the upper rotor's induced velocity. A similar approach was previously used by Sikorsky [28] showed good agreement with experimental results. The inflow equation for the lower rotor is

$$C_{t_l} = 2\lambda_l \sqrt{\mu^2 + (\mu_z - (\lambda_l + \lambda_u))^2} \tag{2}$$

1. *Validation of the Coaxial Rotor Model in Hover*

In order to gain confidence in the coaxial rotor model, the model is compared against "rotor 1" of Harrington's coaxial experimental results [29]. Harrington's "rotor 1" is a two bladed, untwisted rotor with a solidity of 0.054, rotor radius of 3.81m and a separation distance of 9.5% of the rotor diameter. The HGS rotor model is configured to match Harrington's coaxial arrangement and trimmed in the hover state for various thrust coefficients. Figure 2 compares the thrust and torque coefficients of the coaxial model to that of Harrington's experimental results at a rotational speed of 392 ft/s. Also shown in the figure are the results produced by two rotors acting in isolation. These two isolated rotors significantly over predict the thrust and torque produced by the rotor system. However, the results from the coaxial inflow model compare favorably with the experimental results.

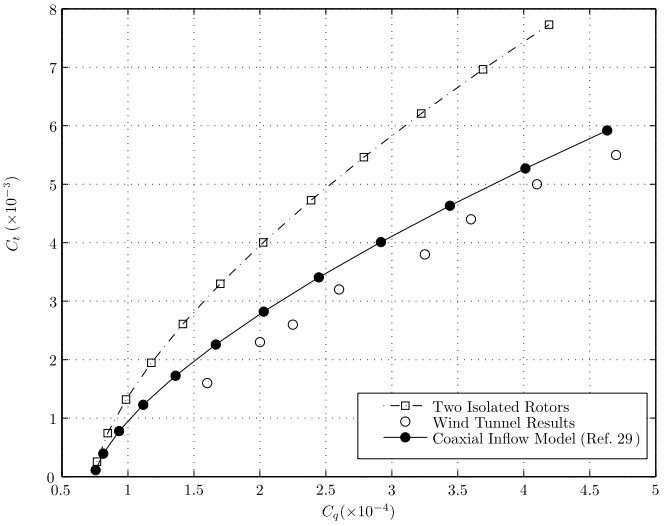

Figure 2. Validation of the Coaxial Rotor Model in Hover

2. *Validation of the Coaxial Rotor Model in Forward Flight*

The coaxial rotor model was compared to performance data of a coaxial rotor in forward flight that was obtained experimentally by Dingeldein [30]. The rotor used in the experiment were identical to that of Harrington's "rotor 1" and the power of the rotor system was measured for various advance ratios. The coaxial rotor system is trimmed for various flight speeds with Figure 3 showing the comparison between Dingeldein's results and the coaxial rotor model. Between advance ratios of 0.1 and 0.2 the coaxial rotor model under predicts the power requirements of the coaxial rotor. As the forward speed increases the wakes of the two rotors begin to skew back [31] and a portion of the upper rotor's wake is not ingested into the lower rotor. This effect is not modeled in the current coaxial rotor model and offers an explanation between the discrepancies with the experimental results. However, the results from the coaxial rotor model do follow the same form as Dingeldein's experimental results and the results appear to come closer as forward speed

increases. The coaxial rotor model appears to compare well with experimental results, particularly at hover and high speeds. This validation gives confidence to the worth of the coaxial rotor results, although a full validation is not possible due to the lack of experimental data.

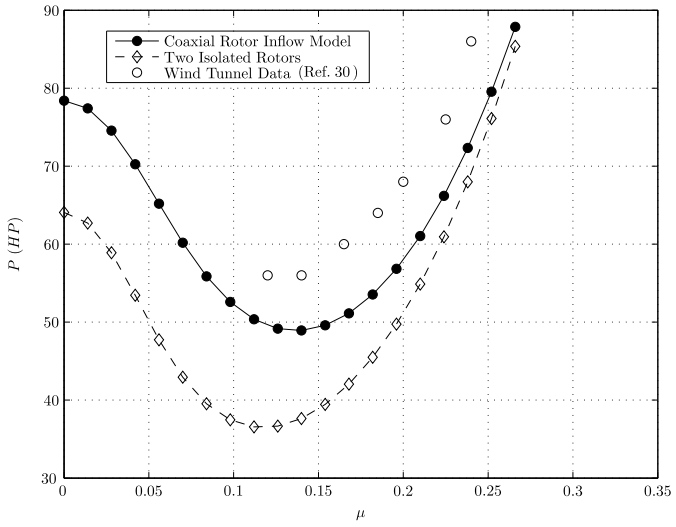

Figure 3. Validation of the Coaxial Rotor Model in Forward Flight

B. Propeller Model

Although it would have been convenient simply to use the existing HGS tail rotor model (re-configured to represent a propeller), there are some fundamental issues. In the derivation of the multi-blade representation of the tail rotor various assumptions are made to cast the equations in closed loop form which are not suitable for a propeller. One of these assumptions is that the magnitude of the tangential velocity of a blade element is much greater than that of the normal velocity. This is suitable for edgewise flow, encountered by a tail rotor, and allows for a small angle assumption, namely that the inflow angle ϕ_i becomes

$$\phi_i = \tan^{-1}\left(\frac{U_p}{U_t}\right) \approx \frac{U_p}{U_t} \tag{3}$$

However, for a propeller this assumption only holds true in low speed flight. In high speed flight the normal velocity, U_p, is composed of the forward flight velocity, therefore the tangential and normal velocities are of similar magnitude violating the small angle assumption. To avoid this an individual propeller blade model was created. The development of the model is very similar to that of the tail rotor with the exception that the loads are calculated through numerical integration and no small angle assumptions are made. Like the main and tail rotor models, the airflow over each blade element is assumed to be two dimensional. The blade element forces and moments are integrated across the propeller span and then around the azimuth to calculate the average forces and moments a propeller blade produces per revolution. These forces and moments are then multiplied by the number of blades to calculate the total forces and moments that the full propeller system produces. Again, like the main and tail rotor models, a dynamic inflow model is used to calculate the induced velocities at each blade element.

C. Wing Model

A simple 2-D representation of the wing using conventional strip theory is used [32]. With the wing located in the vicinity of the main rotor it is necessary to take into account the rotor's wake in the calculation of the incidence of each wing element [33]. The assumption in this wing model is that the induced velocity of the rotor wake does not fully develop when it passes over the wing. The angle of attack at the quarter chord position of each wing element, in body axes is therefore

$$\alpha_w = \theta_{\text{fixed}} + \tan^{-1}\left(\frac{w_w - v_0}{u_w}\right) \tag{4}$$

where u_w and w_w are the tangential and normal velocities of the local strip element, respectively. The local angle of attack of each wing element is then used to calculate the aerodynamic coefficients. The loads are numerically integrated across the wing span to calculate the total forces and moments that the wing produces.

III. Coaxial Compound Configuration

A. Preliminary Design of the Coaxial Compound Helicopter

The coaxial rotor is sized similarly to that of the ABC rotor used on the XH-59A helicopter [34]. The ABC coaxial rotor features very stiff rotor blades [35] to reduce the vertical separation between the rotors and therefore ensure a compact design. A large vertical separation creates some issues by exposing the shaft and control linkages resulting in an increase in parasitic drag at high speeds. Another concern is that a large separation distance would result in the upper rotor creating excessive moments due to the increased distance between its tip path plane and the center of mass. Therefore the CCH model design features very stiff rotor blades that are spaced 0.2R apart, with Table 1 showing the salient design features of the CCH rotor. In terms of the empennage design, the fin's chord is orientated so it is parallel with the fuselage's centreline. Generally, the fin is angled to offload the tail rotor at high speed but this is not required in the CCH model as the upper and lower rotors provide the torque balance. Regarding the control of the CCH model, an extra control is introduced relative to the conventional helicopter. In the CCH model a differential collective control is introduced that allows the pilot to yaw the helicopter. The upper and lower rotor collectives take the form

Table 1. Main Rotor Design of the CCH and BL Models

Characteristic	Baseline Lynx	CCH
R	6.4m	5.49m
Ω	35.8 rad/s	40 rad/s
K_β	166352 Nm/rad	159240 Nm/rad
N_b	4	6
σ	0.077	0.153
γ	7.12	6.57
γ_s	3 deg	3 deg
I_β	678 kgm^2	450 kgm^2
θ_{tw}	-8.02 deg	-10 deg

$$\theta_{\text{u}} = \bar{\theta}_0 + \theta_{\text{diff}} \tag{5}$$

$$\theta_{\text{l}} = \bar{\theta}_0 - \theta_{\text{diff}} \tag{6}$$

Hence, a positive differential collective input increases the blade incidence of the upper rotor whereas it has the opposite effect on the lower rotor, having the net effect of yawing the helicopter's nose to the right. The tail rotor control is replaced by a differential control, θ_{diff}, and a propeller collective control, θ_{prop}, is also introduced resulting in a total of five controls introducing control redundancy into the system. Therefore to trim the CCH model an extra state must be prescribed. Presently, the extra state is the pitch attitude as it directly impacts the thrust that the propeller is required to produce. One possibility is to set a fixed value of pitch to trim the helicopter at all flight speeds, for example $\theta = 0°$, fuselage level. However, this is not always desirable as it would require an excessive level of propeller thrust at certain flight speeds. Another concern is that in low speed flight there is no distinct advantage having the propeller providing thrust as it would unnecessarily increase the overall power consumption of the helicopter. Hence, rather than setting the pitch attitude to a fixed value for all flight speeds, a pitch schedule is developed to minimize the required propulsive force of the propeller. To obtain a pitch schedule the model is passed through an optimization algorithm with Figure 4 showing the optimized pitch attitude and the propeller thrust to trim the CCH from hover up to 200 knots. The magnitude of the propeller thrust is very small until a speed of 60 knots meaning that the coaxial rotor is required to provide the propulsive thrust below 60 knots. However, after 60 knots the coaxial rotor's propulsive duties are shifted to the propeller, with 8 kN of

thrust required at 200 knots. This optimization result aids the design of the propeller with Table 2 showing the chosen design parameters of the propeller. The rotational speed is chosen to provide a high velocity airflow over the propeller blades without compressibility effects becoming an issue at high speeds. The propeller also features Clark Y airfoils along the span with a high level of twist so that each propeller blade element operates at a favorable angle of attack [36].

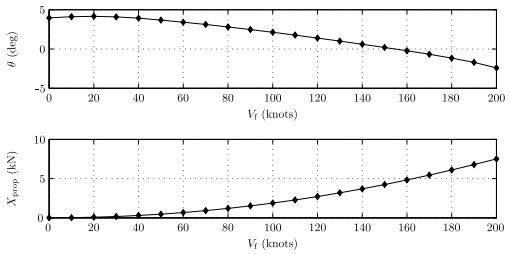

Figure 4. Optimisation of the CCH Model

Table 2. Propeller Design of the CCH Model

Design Parameter	CCH
R_{prop}	1.4m
Ω_{prop}	207 rad/s
θ_{tw}	-30 deg
σ_{prop}	0.142
$\mathbf{x}_{\text{prop}}$	(-7.66, 0, 0)m

Another design concern with compound helicopters is that compressibility effects at the advancing blade tip can be an issue in high speed flight. If the Mach number of the advancing blade tip reaches 0.91, then a portion of the local airflow becomes supersonic leading to the formation of shock waves, thereby resulting in a significant increase of drag [37]. The solution is to slow the main rotor at high speeds, for example the Sikorsky X2's coaxial rotor is slowed by 20% at high speeds [5]. In a design analysis of a compound helicopter, Yeo and Johnson slowed the main rotor considerably, from a blade tip speed of 750 ft/s in hover to being slowed to 502 ft/s in the helicopter's cruise condition of 250 knots, so that the advancing tip Mach number was 0.8 in cruise [38]. Unfortunately, the level of modeling taken with this present study prohibits the assessment of the compound helicopters at these very high speeds (above 200 knots). As mentioned previously, the current rotor model does not properly model the highly nonlinear aerodynamic phenomena which can be expected at very high speeds. However, with the assumption that 200 knots is the CCH configuration's forward speed boundary, it is necessary to reduce the rotational speed of the coaxial rotor to avoid the advancing tip Mach number approaching drag divergence. Above 140 knots the rotational speed of the coaxial rotor is reduced, with Figure 5 showing both the variation of the rotorspeed and advancing tip Mach number. At 200 knots the coaxial rotor has slowed by 13% and therefore successfully avoids the Mach tip number of 0.91, whereby compressibility effects become an important issue.

B. Trim Results of the Coaxial Compound Helicopter

Figure 6 shows the trim results of the CCH and BL models. In the hover, the coaxial inflow model, equations (1) and (2), result in higher induced velocities through the lower rotor than that of the upper rotor. Therefore, the induced power loss of the lower rotor is greater than the upper rotor, if the upper and lower thrust coefficients are equal. Hence, to provide a torque balance the upper rotor must create more thrust than the lower rotor to match the lower rotor's torque, with the thrust sharing ratio of the upper and lower rotors being 1.32 in the hover. Another consequence of the higher induced velocities of the lower rotor is the reduced blade incidence of the lower rotor blades if $\theta_u = \theta_l$. Therefore to compensate for the strong inflow through the lower rotor, the lower rotor's collective is slightly higher than that of upper rotor in low speed flight. This partitioning of the rotor thrusts and the higher pitch of

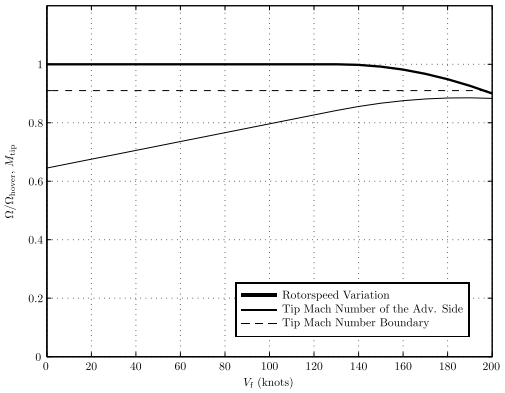

Figure 5. CCH Configuration's Variation of Rotorspeed

the lower rotor are both consistent with findings from other trimmed coaxial rotors in hover [27, 39, 40]. As the CCH model moves away from hover the thrust sharing ratio tends towards unity and θ_{diff} tends towards zero as the aerodynamic interference between the rotors lessen as μ begins to dominate the coaxial inflow equations (1) and (2).

Another interesting feature of the trim results is the difference between the lateral cyclic required for both models. In a conventional helicopter a large amount of lateral cyclic is required between 0 - 50 knots, as can be seen with the BL model. As the conventional helicopter moves into forward flight the rotor wake skews backwards lowering blade incidence at the rear of the rotor disc. This effect causes the helicopter to roll to starboard (for a helicopter rotor that rotates anti-clockwise when viewed from above). In order to counteract this rolling moment a large amount of lateral cyclic is required to trim the helicopter. This effect still exists in the coaxial rotor but the two rotors flap in opposite directions requiring little lateral cyclic. For speeds above 150 knots, the propeller produces the majority of the axial thrust requiring a small amount of lateral cyclic, θ_{1c}, to balance the propeller torque. The lack of tail rotor and the fin not being angled relative to the fuselage centerline reduces the side force that the helicopter produces from hover to 200 knots which consequently reduces the bank angle of the fuselage significantly. There is little difference between the two longitudinal cyclic results (negative longitudinal cyclic tilts the rotor disc forward) until a flight speed of approximately 80 knots. After this flight speed the propeller begins to provide axial thrust reducing the longitudinal cyclic required.

IV. Hybrid Compound Configuration

A. Preliminary Design of the Hybrid Compound Helicopter

The HCH model features both wing and thrust compounding with the two propellers fulfilling the dual purpose of providing the anti-torque moment and propulsive thrust whereas the wing offloads the main rotor at high speeds. Like the CCH model, it is necessary to take into account some design considerations. The main design task is the sizing of propellers and wing. The addition of a wing to any compound helicopter configuration degrades hover performance by creating aerodynamic download and additional structural weight. The download and extra weight must be compensated with an increase in rotor thrust and an increase in power consumption. To retain good VTOL capability the wing must be sized in a manner that does not adversely reduce hover performance whilst having the ability to offload the main rotor at high speeds.

Another complication is that the sizing of the wing influences the design of the propellers. As mentioned previously, the propellers are required to provide the anti-torque moment in low speed flight. The propellers are mounted on the outer sections of the wing to provide adequate clearance between the propeller blades and the fuselage. It is clear that a greater wing span will result in lower propeller thrusts required to provide the anti-torque moment as the lever arm from the propeller to the center of mass is increased. The selected wing area for the HCH model is 12m^2 with an aspect ratio of 6. This wing area can

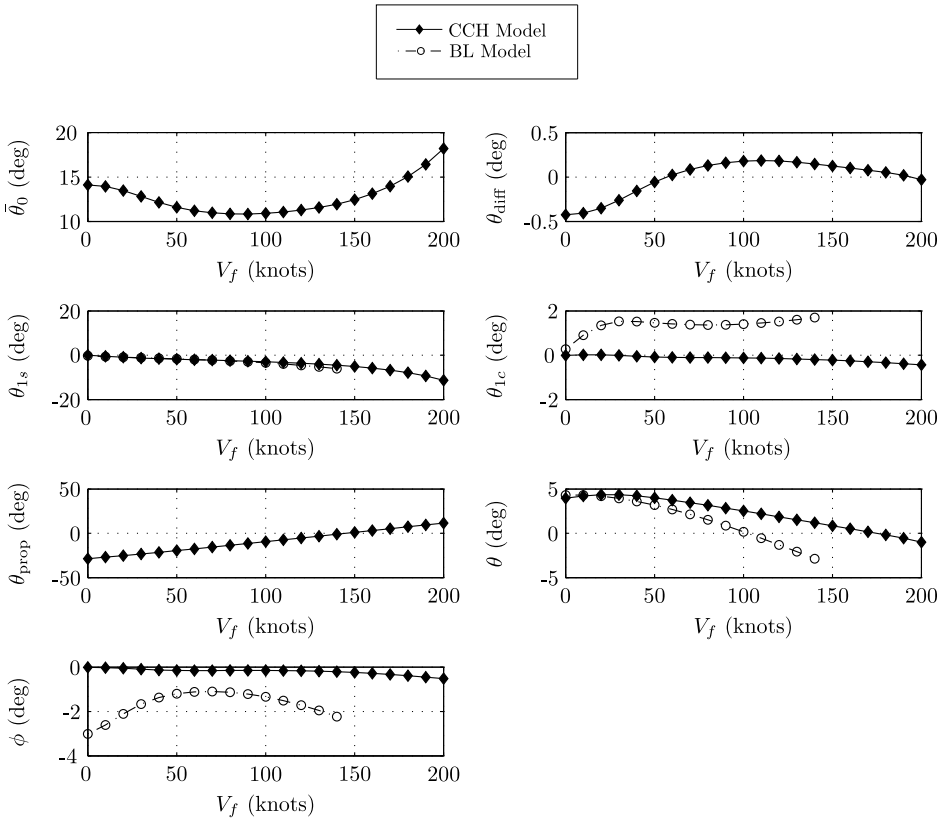

Figure 6. Trim Results of the CCH Model

create a significant amount of lift at high speed without adversely degrading hover performance. Also this combination of the wing area and aspect ratio creates a sizable lever arm between the propellers and the center of mass thus reducing the propeller thrusts at low speed flight. In terms of the aspect ratio, a value of 6 is chosen because a higher aspect ratio would lead to a wing span that would extend further into the higher velocities of the rotor wake whereas a lower aspect ratio would result in a greater induced drag penalty [41]. A choice of 6 is an appropriate compromise between these two effects and has been used on various winged helicopters [10, 42]. Also the moment of inertia around the x axis, I_{xx}, has been slightly increased to account for the offset mass of the wing from the center of gravity.

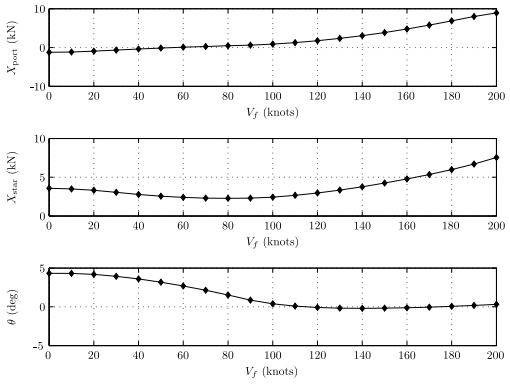

Figure 7. Optimisation Results of the HCH Model

Concerning the control of the HCH model, a mean propeller collective setting controls the magnitude of the two propeller thrusts whereas a differential propeller collective controls the yawing motion of the helicopter. The starboard and port propeller collectives take the from

$$\theta_{\text{star}} = \bar{\theta}_{\text{prop}} + \theta_{\text{diff}} \tag{7}$$

$$\theta_{\text{port}} = \bar{\theta}_{\text{prop}} - \theta_{\text{diff}} \tag{8}$$

The differential propeller setting, θ_{diff}, mean propeller collective, $\bar{\theta}_{\text{prop}}$, as well as the standard main rotor collective and cyclic controls result in five controls. As with the CCH model the extra state that is controlled is the pitch attitude. In this design controlling the pitch attitude is particularly useful as it allows for direct control of the wing lift. In a similar manner to the CCH model, the model is passed through an optimization algorithm to develop a pitch schedule for the HCH model that reduces the required propeller thrusts. It should be noted that the HCH model could, in theory, be trimmed with a pitch attitude of zero at all flight speeds but there is an important issue that arises in low speed flight. In order to trim the HCH model in the hover, at a pitch attitude of zero, a large amount of negative thrust is required from the port propeller. As forward speed increases and the port propeller continues to create large amounts of negative thrust, to maintain a level fuselage, the forward velocity and the induced velocity of the port propeller travel in opposite directions. When their magnitudes are similar there would be no well defined slipstream and eventually the vortex ring state would be reached at some flight speed, resulting in the solutions from momentum theory being no longer valid [43]. Hence the pitch attitude is scheduled in such a manner that avoids the port propeller providing large amounts of negative thrust in low speed flight. Figure 7 shows the pitch schedule and propeller thrusts that are required from hover up to a flight speed of 200 knots. It was originally found that this manner of pitch scheduling does impose the penalty of increasing the pitch attitude in the hover, from 4.3° for the BL model to 8.4° for the HCH model. The reason for this increase in pitch attitude is that the starboard propeller provides a significant thrust to provide the anti-torque moment and the main rotor flaps backwards to oppose this force. However, this high pitch attitude setting in low speed flight can be attenuated by an appropriate selection of the rotor shaft tilt. Selecting a shaft tilt angle, γ_s, of zero results in the pitch schedule shown in Figure 7. For the trim problem, the pitch

attitude is set close to zero after 150 knots to maximize the lift produced by the wing. A combination of setting the pitch attitude to zero after 150 knots as well as a fixed wing pitch setting of 5° maximizes the lift of the wing whilst maintaining an adequate stall margin. Again, the optimization results aid the propellers design by showing the thrusts required. The starboard and port propellers are identical with the exception that they rotate in opposite directions with Table 3 showing the important design properties of the propellers.

Table 3. Propeller Design of the HCH Model

Design Parameter	HCH
R_{prop}	1.3m
Ω_{prop}	207 rad/s
θ_{tw}	-30 deg
σ_{prop}	0.153
$\mathbf{x}_{\text{prop}}$	(0.05, $\pm$3.87, 0.13)m

Similar to that of the CCH configuration, it is necessary to slow the HCH configuration's main rotor to avoid compressibility effects. After 140 knots, the main rotor's speed is gradually lowered to avoid drag divergence. At 200 knots the main rotor is slowed to 83.8%, see Figure 8, thereby avoiding an advancing tip Mach number of 0.91 which is assumed to be limit before drag divergence occurs.

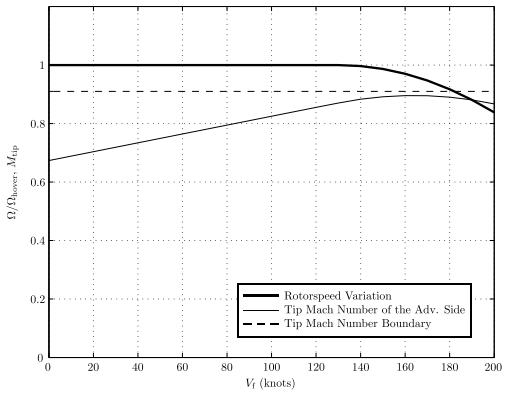

Figure 8. HCH Configuration's Variation of Rotorspeed

B. Trim Results of the Hybrid Compound Helicopter

The trim results of the HCH model and the BL model are shown in Figure 9. The first result to note is the difference between the collective settings. As the speed approaches 80 knots, the collective setting of the HCH model begins to reduce as the wing begins to offload the main rotor whereas with the BL model the collective begins to increase tending towards the limiting case of retreating blade stall. There is little difference between the longitudinal cyclic values of the two models until 120 knots. However, after 120 knots, the two propellers begin to supply the propulsive force and therefore the rotor disc is no longer required to be tilted forward to provide the propulsive force but to maintain the pitch attitude required. There is less lateral cyclic required in the hover due to the rotor not having to produce a side force to counteract the tail rotor. The lateral cyclic results of the two models are of similar form throughout the speed range. In terms of the attitudes, the absence of a tail rotor reduces the bank angle of the fuselage for all flight speeds. The differential propeller collective is at its highest in low speed flight to provide the anti-torque moment. As forward speed increases, the anti-torque moment duties are shifted towards the fin as it provides a side force which results in the propeller differential setting lowering as speed increases. At flight speeds in excess of 150 knots, the main rotor controls alter significantly due to the reduction of the main rotor's speed, in order to avoid compressibility effects. Hence, the wing offloads the main rotor to a greater extent with the rotor producing only 10% of the overall vehicle lift at 200 knots. At this flight speed it is possible that the control of the vehicle would transition from main rotor controls to fixed wing controls, similar to that of a tilt-rotor aircraft, with conventional aircraft controls such as as ailerons, elevator and a rudder.

Figure 10 compares the trim results of the CCH and HCH models. The main rotor collective of the CCH model is of similar form to a conventional helicopter. Whereas the collective of the HCH model lowers after 80 knots due to the wing offloading the main rotor. The longitudinal cyclics of the two models are similar. The form of lateral cyclic of the HCH model is analogous to that of a conventional helicopter whereas with the CCH model the lateral cyclic required is very small due to the coaxial rotor arrangement. In terms of the propeller controls, the results match very closely and linear with flight speed. Concerning the pitch attitudes of the two helicopters, the pitch attitude of the CCH model is higher than the HCH model between 60-140 knots as the main rotor flaps back to oppose the propeller thrust that provides the propulsive force. With the CCH model, in low speed flight the pitch attitude is similar to a conventional helicopter as the propeller does not produce any meaningful axial thrust. The roll angle of the CCH model is very small at all flight speeds as the empennage design produces little side force in trim as the coaxial rotor system provides the torque balance. Whereas the roll angle of the HCH model is slightly higher than the CCH model due to the side force that the fin produces.

V. Dynamic Stability of the Two Compound Configurations

The two compound helicopter models have been trimmed and the next logical step is assessing their dynamic stability. All the helicopter models that are presented within the paper take the non-linear form of

$$\dot{\mathbf{x}} = \mathbf{f}(\mathbf{x}, \mathbf{u}) \tag{9}$$

Using small perturbation theory, equation (9) can be reduced to the linearized form of

$$\dot{\mathbf{x}} = \mathbf{A}\mathbf{x} + \mathbf{B}\mathbf{u} \tag{10}$$

where $\mathbf{A}$ and $\mathbf{B}$ are known as the system and control matrices. Due to the complex nature of the non-linear equations of motion for these helicopters the equations are reduced to linear form using a numerical linearization algorithm [44]. Using this technique the system and control matrices can be formed at various trimmed conditions. Furthermore, the eigenvalue values of the system matrix give the natural modes of motion at that particular flight condition. Using these techniques, a dynamic stability analysis of each compound helicopter is performed from hover to 200 knots.

A. Predicted Dynamic Stability of the CCH Configuration

Figure 11 shows the roll subsidence, pitch subsidence and dutch roll modes of both the BL and CCH configurations. All three of these modes exhibit stability for both helicopter models. The damping of the roll subsidence mode of the CCH configuration has increased slowing the roll response of the aircraft. The reason for this is due to a combination of the increased number of rotor blades, their stiffness and the increased distance between the upper rotor's hub and the center of gravity. The level of roll damping is given by L_p and for the CCH configuration is insensitive to flight speed with it being approximately -16 $(1/s)$.

In terms of the dutch roll mode, the main difference is the frequency of the two modes, with the CCH configuration exhibiting a smaller frequency, at high speeds, due to its empennage design. This can be seen by using Padfield's [17] approximation to the dutch roll mode frequency in high speed flight

$$\omega_{\text{dr}}^2 \approx U_e N_v + L_v \left(\frac{g - N_p U_e}{L_p} \right) \tag{11}$$

The reduced dutch roll frequency of the CCH model is due to the Weathercock stability derivative N_v. For a conventional helicopter N_v is generally positive for most flight speeds with the tail rotor and fin playing the most prominent roles. Following a sideslip perturbation the fin and tail rotor provide a side force that aligns the fuselage nose with the wind direction, thus providing a stabilizing effect. However,

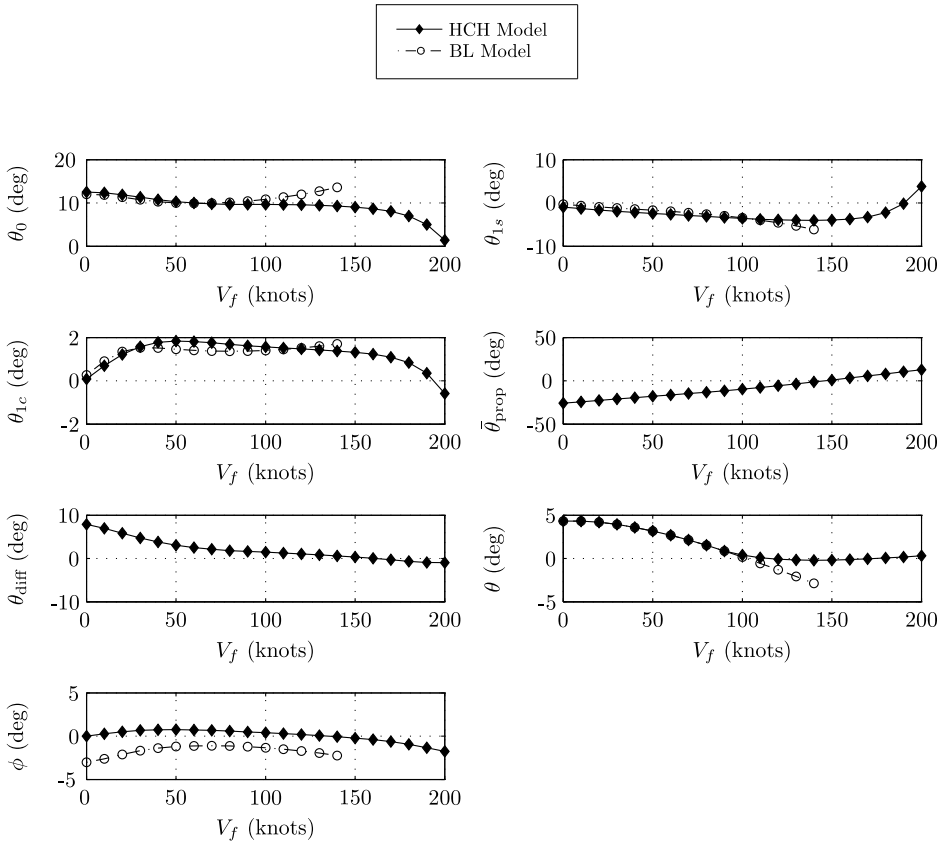

Figure 9. Trim Results of the HCH Model

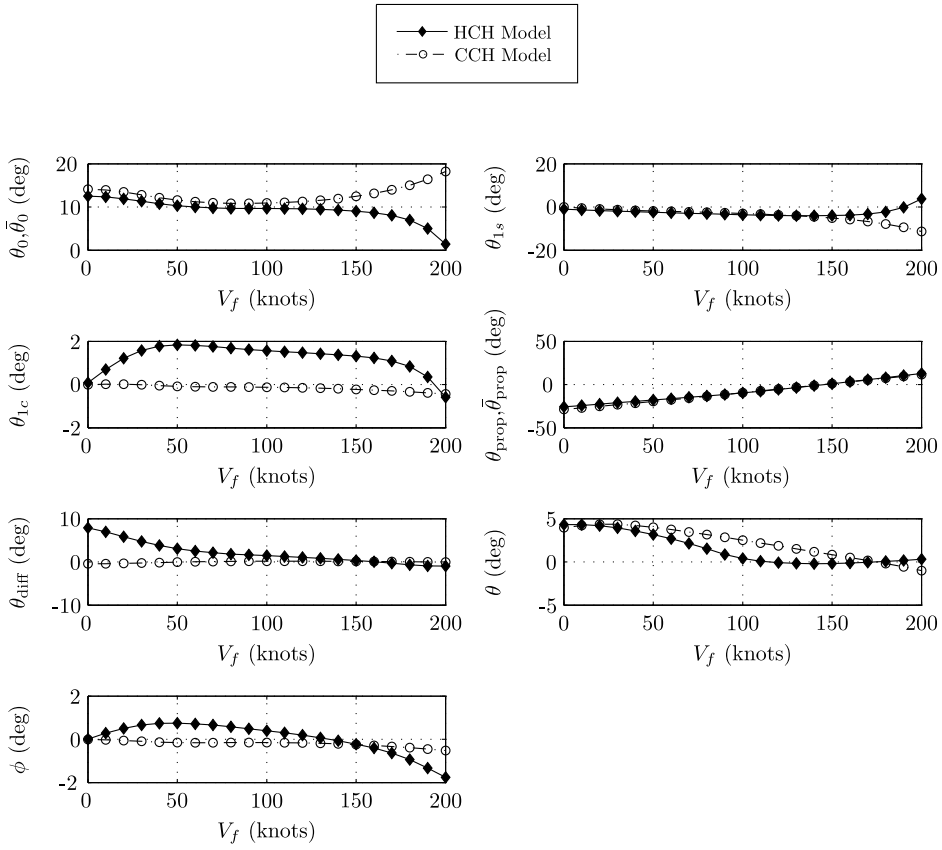

Figure 10. Trim Results of the HCH and CCH Models

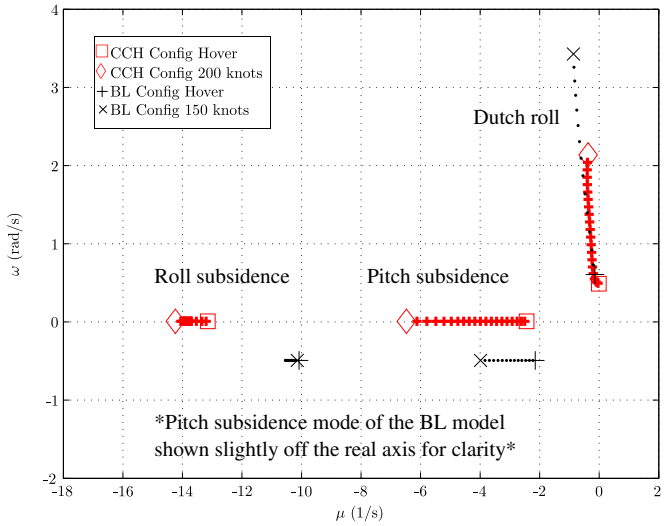

Figure 11. Roll Subsidence, Pitch Subsidence and Dutch Roll Modes of the CCH and BL Models

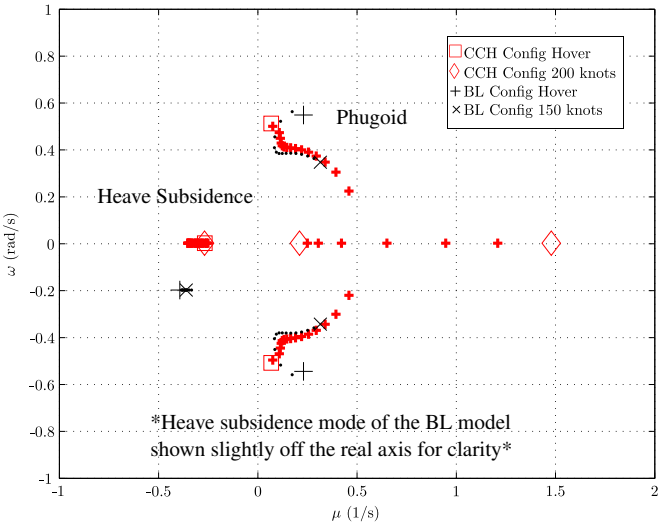

Figure 12. Phugoid and Heave Subsidence Mode of the CCH and BL Models

for the CCH configuration this derivative is destabilizing for all flight speeds due to the combination of the lack of tail rotor and the fin not being angled relative to the fuselage centreline. These two design features reduce the yawing moment that the helicopter produces following a sideslip perturbation. The fuselage is now the main contributor to N_v which provides a destabilizing moment following a sideslip perturbation due to the fuselage's aerodynamic center being located fore of the center of gravity position. In forward flight, equation (11) shows that a negative value of N_v reduces the dutch roll frequency which can be seen in Figure 11.

Figure 12 shows the phugoid and heave subsidence modes of the BL and CCH models. The phugoid mode for both the BL and CCH models are of similar form but the CCH model's eigenvalues are shifted closer to the imaginary axis in low speed flight. Indeed, the phugoid mode of the CCH model is predicted to be neutrally stable in low speed flight before becoming unstable. These two models feature hingeless rotor systems and this is the primary reason for the instability [45]. The stiff rotors create large moments around the rotor hub due to the stiffness of the blades and large effective hinge offset. When the two helicopters are subject to a perturbation in forward speed, the two rotor systems flap backwards resulting in the fuselage pitching up. As the fuselage pitches up, the main rotor provides a pitch down moment, with the stability derivative M_q being negative, with this oscillatory motion continuing with the amplitude steadily increasing. As mentioned previously, the phugoid mode of the CCH model is close to the imaginary axis, in low speed, due to an increase in drag damping. Following a perturbation in forward speed the blade incidence of the propeller blades reduce providing an extra drag force, lowering the value of X_u, but this is still insufficient to stabilize the phugoid. Regarding the heave subsidence mode, there is little change between the two models. It should be noted that the eigenvalues of the spiral mode for all models are not shown within the presented results as their eigenvalues are very similar, with the eigenvalues being small and negative indicating stability for all the models.

B. Predicted Dynamic Stability of the HCH Configuration

Figure 13 shows the roll subsidence, pitch subsidence and dutch roll modes of both the BL and HCH models. Firstly, consider the roll subsidence mode. For the BL model the roll damping does not change significantly from hover to 150 knots and is dominated by the stiffness of the rotor. However, the roll damping eigenvalues of the HCH model range from -8 $(1/s)$ in the hover to -17 $(1/s)$ at 200 knots. In the HCH model the structural weight of the wing creates a greater moment of inertia around the x axis than that of the BL helicopter. Although the stiffness properties remain the same for these two helicopter rotors, the HCH model's roll damping is scaled by I_{xx} thus resulting in a lower value of L_p in the hover. As speed increases the lift produced by the wing increases and the damping of the roll mode also increases. At high speeds, the wing is producing a significant portion of the overall lift of the helicopter. In a fixed wing aircraft the roll mode is always stable as a positive perturbation in roll rate increases the angle of attack of the starboard wing and decreases the angle of attack of the port wing [46], thus producing a stabilising rolling moment. This effect also occurs in the HCH model and is now added to the roll damping produced by the hingeless rotor.

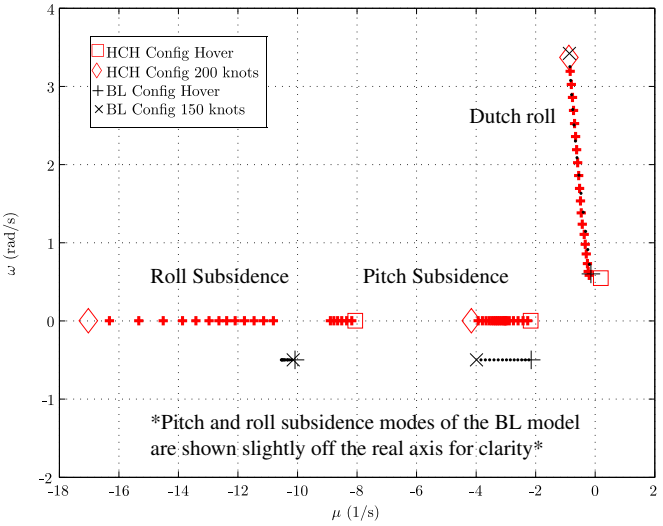

Figure 13. Roll Subsidence, Pitch Subsidence and Dutch Roll Modes of the HCH and BL Model

In terms of the short period modes, there is little change between the eigenvalues of both the HCH and BL configurations. The eigenvalues of the short period modes are primarily influenced by the stability derivatives Z_w,M_q and M_w. Padfield [17] approximates the characteristic equation of the short period modes as

$$\lambda_{sp}^2 - (Z_w + M_q)\lambda_{sp} + Z_w M_q - M_w(Z_q + U_e) = 0 \qquad (12)$$

In terms of the HCH model, at high speeds, the stability derivative M_w decreases, relative to the BL model. The reason for the attack of angle stability derivative, M_w, decreasing is due to the contribution of

the wing . The quarter chord position of the wing is slightly aft of the centre of gravity position. Therefore, after a perturbation in normal velocity the wing produces a negative pitch down moment which opposes the main rotor contribution to M_w. This combination creates a canceling effect between the main rotor and the wing which results in M_w becoming small at 200 knots, with Equation (12) giving an accurate approximation to the short period eigenvalues for all flight speeds. For example, at 200 knots, for the HCH model M_q = -3.217 $(1/s)$, Z_w = -1.792 $(1/s)$ and M_w = 0.0196 (rad/s.m), which agree favourably with the eigenvalues presented in Figures 13 and 14.

Figure 14 shows the phugoid and heave subsidence modes of the HCH and BL models. In the hover, the phugoid modes of the HCH and BL models are similar. However, as speed increases the mode becomes stable for the HCH model but with decreasing frequency. Therefore the phugoid tends towards an exponential mode rather than the oscillatory mode of the BL model. The oscillatory nature of the mode is reduced due to the contribution of M_u with this derivative tending towards zero above 160 knots. This derivative is analogous to M_w with the wing providing a cancellation of the pitch up moment produced by the main rotor following a perturbation of forward speed. The net effect is that the ratio of the pitching moment due to speed and pitch rate becomes very small lessening the oscillatory nature of the phugoid. At 160 knots the eigenvalues of the phugoid mode branch off into the real axis and produce a purely divergent mode. In a real aircraft this would be viewed as a flying qualities issue and it is likely that the flight control system would be configured to improve the aircraft's phugoid characteristics. Concerning the damping of the mode, after 80 knots the phugoid becomes stable due to the drag damping derivative, X_u. For a conventional helicopter X_u is always negative as a perturbation in forward velocity results in an increase in drag force due to the fuselage and the rotor disc tilting backwards. However, for the HCH model, the drag is increased following a perturbation in forward velocity due to the addition of the two propellers and wing. A perturbation in forward velocity reduces the blade incidence of the propeller blades which creates a sizable drag force. Additionally, the perturbation of u also increases the drag of the wing, hence both contribute to lower the drag damping derivative, X_u, which in turn stabilizes the phugoid.

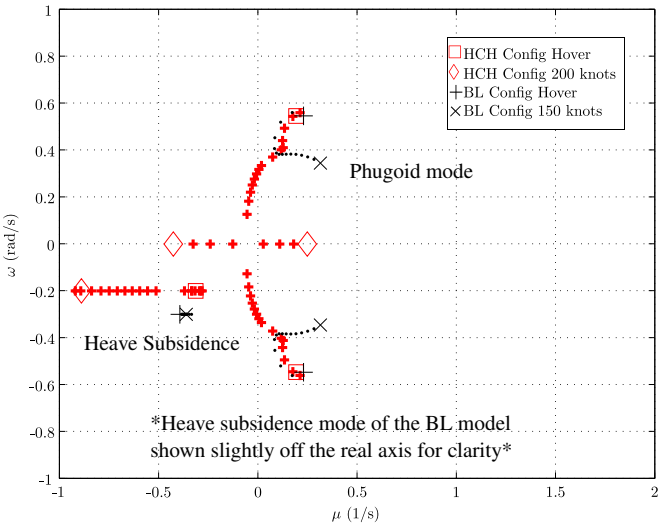

Figure 14. Phugoid and Heave Subsidence Modes of the HCH and BL Model

Figure 15 shows the comparison between the roll subsidence, pitch subsidence and dutch roll modes of the CCH and HCH configurations. The roll damping of the CCH model is insensitive to flight speed whereas the flight speed has a profound influence with regards to damping of the HCH model. The roll damping of the HCH model is at its lowest in the hover and increases with flight speed due to the wing providing a large portion of the vehicle lift. Regarding the dutch roll modes, both models predict a lightly damped mode with the main difference being the frequencies of the two modes. As for the short period modes, the eigenvalues of the HCH model's heave and pitch subsidence modes are approximated with Equation (12). For a conventional helicopter in high speed flight, the derivative M_w significantly influences the eigenvalues of the short period modes, as seen in Equation (12). However, for the HCH model, M_w plays a lesser role in determining the eigenvalues of the short period modes. With regards to the CCH model, the stability derivative M_w becomes increasingly significant at high speeds influencing the heave and pitch subsidence modes. Similar to that of the BL model, the contribution of M_w results in the heave and pitch subsidence eigenvalues being well separated throughout the speed range.

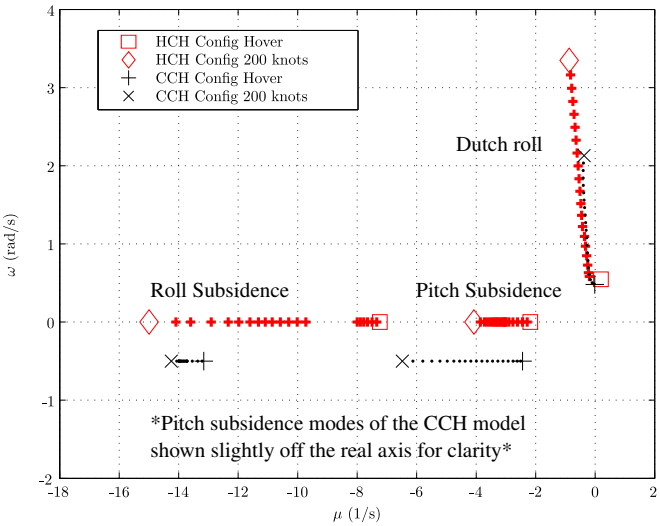

Figure 15. Roll Subsidence, Pitch Subsidence and Dutch Roll Modes of the CCH and HCH Models

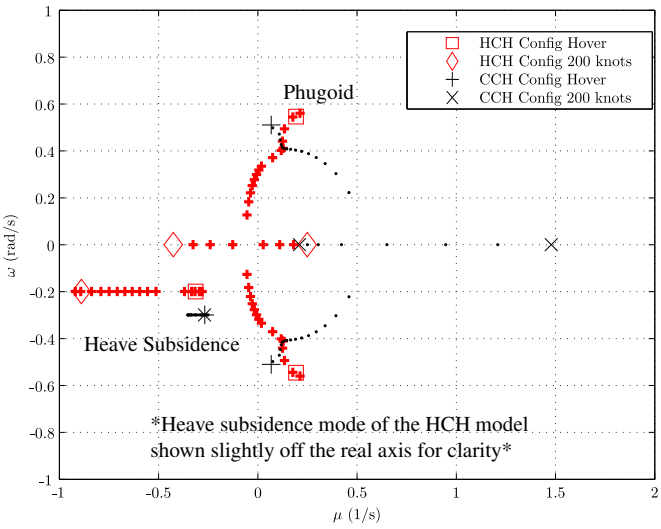

Figure 16. Phugoid Modes of the CCH and HCH Models

Figure 16 shows the phugoid and heave subsidence modes of the CCH and HCH models. The phugoid mode of the HCH configuration becomes stable after 80 knots due the increased drag following a perturbation of forward speed. However, the oscillatory nature of the mode is reduced due to the wing providing a stabilizing moment following a perturbation of forward velocity. Whereas the form of the phugoid mode of the CCH model is similar to that of the BL model but the eigenvalues are shifted closer to the imaginary axis, in low speed flight. For the CCH model, the stability derivative M_u is positive for all flight speeds as a perturbation of forward speed results in the rotor disc

flapping backwards thus producing a pitching up motion and therefore oscillatory response. The propeller of the CCH model does contribute to reduce the drag damping derivative X_u, but its contribution is incapable of stabilizing the phugoid. The eigenvalues of both the HCH and CCH models do eventually reach the axis and hence predict purely divergent modes. Therefore is seems likely that a SAS would be required to stabilize the phugoid modes for both aircraft at high speeds.

VI. Conclusions

Two compound helicopter models have been developed and their trim and dynamic stability has been compared to a conventional helicopter. The main conclusions from the current work are as follows:

1. A coaxial rotor model has been developed and has been partially validated with experimental results. The results show good agreement in the hover and at high speed flight but due to a lack of experimental data a full validation is not possible.

2. The trim results of the CCH model show that little lateral cyclic control is required to trim the helicopter. Also the omission of a tail rotor in the design significantly reduces the bank angle of the fuselage across the speed range.

3. The trim results of the HCH model show a reduction of collective required after 80 knots as the wing begins to offload the main rotor. The differential propeller collective control required is at its highest in low speed flight but reduces as flight speed increases as the fin provides the anti-torque moment. There is also less longitudinal cyclic required after 120 knots as the propellers provide the propulsive force.

4. The main differences between the natural modes of motion of the CCH and BL configurations are the dutch roll and roll subsidence modes. The frequency of the dutch roll mode is less than that of the BL mode due to the lack of tail rotor and a reduced side force contribution from the fin, following a sideslip perturbation. The differences between the roll modes is primarily due to the design of the main rotor systems. The increased number of rotor blades, their respective stiffness and the increased distance between the upper rotor's hub to the center of gravity position all contribute to increasing the roll damping, relative to the BL model.

5. The main differences between the HCH and BL modes of motion were the phugoid and roll subsidence modes. The phugoid becomes stable for the HCH model due to the increase in drag damping, a reduced X_u, however the mode tends towards an aperiodic response due the canceling effect of pitching moments between main rotor and wing. This is because the wing provides a pitch down moment following a perturbation in angle of attack since its quarter chord position is slightly behind the center of mass. Therefore, the positioning of the wing can strongly influence the phugoid mode of the helicopter. Concerning the roll subsidence mode, the damping of the mode increases with flight speed due to the additional roll damping the wing provides.

This paper has investigated the dynamic stability of compound helicopter configurations, however it must be stressed that more work has to be done to fully investigate the compound configuration. One area for future work relates to the control of the compound helicopter and how the additional control(s) could be utilized during standard helicopter maneuvers to maximize performance. This would naturally lead to a handling qualities assessment of these aircraft and how the pilot workload is affected by this additional control. These studies would assist the design of the compound helicopter and could perhaps reinforce the potential of the compound helicopter.

Acknowledgements

The authors would like to acknowledge the Scottish Funding Council (SFC) for providing the funding, under the GRPE Scholarship, to conduct this research.

References

[1] M.N. Orchard and S.J. Newman. The compound helicopter - why have we not succeeded before? *The Aeronautical Journal*, 103(1028):489–495, 1999.

[2] J.G. Leishman. *Principals of Helicopter Aerodynamics*. Cambridge University Press, 2nd edition, 2006. ISBN 978-0-521-85860-1.

[3] R.K. Burgess. The ABC Rotor - A Historical Perspective. In *American Helicopter Society 60th Annual Forum*, Baltimore, MD, 2004.

[4] A. Bagai. Aerodynamic Design of the X2 Technology Demonstrator Main Rotor Blade. In *American Helicopter Society 64th Annual Forum*, Montreal, Canada, 2008.

[5] R. Blackwell and T. Millott. Dynamics Design Characteristics of the Sikorsky X2 Technology Demonstrator Aircraft. In *American Helicopter Society 64th Annual Forum*, Montreal, Canada, 2008.

[6] D. Walsh, S. Weiner, A. Bagai, T. Lawerence, and R. Blackwell. Development Testing of the Sikorsky X2 Technology Demonstrator. In *American Helicopter Society 65th Annual Forum*, Grapevine, TX, 2009.

[7] P.J. Arcidiacono, G. DeSimone, and J. Occhiato. Preliminary Evaluation of RSRA Data Comparing Pure Helicopter, Auxiliary Propulsion and Compound Helicopter Flight Characteristics. In *American Helicopter Society 36th Annual Forum*, pages 42–51, Washington D.C., 1980.

[8] F.P. Lentine, W.P. Groth, and T.H. Oglesby. Research in Maneuverability of the XH-51A Compound Helicopter. USAAVLABS Technical Report 68-23, 1968.

[9] R.W. Prouty. The Lockheed Helicopter Experience. In *American Helicopter Society 65th Forum*, Grapevine, TX, 2009.

[10] R.C. Dumond and D.R. Simon. Flight Investigation of Design Features of the S-67 Winged Helicopter. *Journal of the American Helicopter Society*, 18(3):2–9, 1973. doi: 10.4050/JAHS.18.2.

[11] M. Orchard and S.J. Newman. The fundamental configuration and design of the compound helcopter. *Proceedings of the Institution of Mechanical Engineers, Part G: Journal of Aerospace Engineering*, 217(6):297–315, 2003. doi: 10.1243/095441003772538570.

[12] M.K. Sekula and F. Gandhi. Effects of Auxiliary Lift and Propulsion on Helicopter Vibration Reduction and Trim. *Journal of Aircraft*, 41(3):645–656, 2004. doi: 10.2514/1.496.

[13] R.W. Prouty. *Helicopter Performance, Stability, and Control*. Robert E. Krieger Publishing Company, Inc., reprint edition, 1990.

[14] M. Orchard and S.J. Newman. Some design issues for the optimisation of the compound helicopter configuration. In *American Helicopter Society 56th Annual Forum*, Virginia Beach, VA, 2000.

[15] M.Buhler and S.J. Newman. The Aerodynamics of the Compound Helicopter Configuration. *The Aeronautical Journal*, 100(994):111–120, 1996.

[16] S.S. Houston. The Gyrodyne - A Forgotten High Performer? *Journal of the American Helicopter Society*, 52(4):382 – 391, 2007. doi: http://dx.doi.org/10.4050/JAHS.52.382.

[17] G.D. Padfield. *Helicopter Flight Dynamics: The Theory and Application of Flying Qualities and Simulation Modelling*. Blackwell Science, 1996. ISBN 0-632-03248-0.

[18] D.G. Thomson. Development of a Generic Helicopter Mathematical Model for Application to Inverse Simulation. Internal Report No. 9216, Department of Aerospace Engineering, University of Glasgow, UK, 1992.

[19] S. Rutherford. *Simulation Techniques for the Study of Advanced Rotorcraft*. Phd, University of Glasgow, 1997.

[20] S. Doyle and D.G. Thomson. Modification of a helicopter inverse simulation to include an enhanced rotor model. *AIAA Journal of Aircraft*, 37(3):536 – 538, 2000. doi: 10.2514/2.2633.

[21] R. Bradley, G.D. Padfield, D.J. Murray-Smith, and D.G. Thomson. Validation of helicopter mathematical models. *Transactions of the Institute of Measurement and Control*, 12(186), 1990. doi: 10.1177/014233129001200405.

[22] D.M. Pitt and D.A. Peters. Rotor Dynamic Inflow Derivatives and Time Constants from Various Inflow Models. In *9th European Rotorcraft Forum*, Stresa, Italy, 1983.

[23] R.T.N. Chen. A Survey of Nonuniform Inflow Models for Rotorcraft Flight Dynamics and Control Applications. NASA TM 102219, 1989.

[24] J.G. Leishman and M. Syal. Figure of Merit Definition for Coaxial Rotors. *Journal of the American Helicopter Society*, 53(3):290–300, 2008. doi: 10.4050/JAHS.53.290.

[25] J.G. Leishman and S. Ananthan. An Optimum Coaxial Rotor System for Axial Flight. *Journal of the American Helicopter Society*, 53(4):366–381, 2008. doi: 10.4050/JAHS.53.366.

[26] H.W. Kim and R.E. Brown. A Rational Approach to Comparing the Performance of Coaxial and Conventional Rotors. *Journal of the American Helicopter Society*, 55(1):012003, 2010. doi: 10.4050/JAHS/55.012003.

[27] H.W. Kim and R.E. Brown. A Comparison of Coaxial and Conventional Rotor Performance. *Journal of the American Helicopter Society*, 55(1): 012004, 2010. doi: 10.4050/JAHS.55.01.2004.

[28] V.M. Paglino. Forward Flight Performance of a Coaxial Rigid Rotor. In *American Helicopter Society 27th Annual Forum*, Washington D.C., 1971.

[29] R.D. Harrington. Full-Scale-Tunnel Investigation of the Static-Thrust Performance of a Coaxial Helicopter Rotor. NACA TN-2318, 1951.

[30] R. Dingeldein. Wind-Tunnel Studies of the Performance of Multirotor Configurations. NACA TN 3236, 1954.

[31] A. Bagai and J.G. Leishman. Free-Wake Analysis of Tandem, Tilt-Rotor and Coaxial Rotor Configurations. *Journal of the American Helicopter Society*, 41(3):196–207, 1995. doi: 10.4050/JAHS.41.196.

[32] Christopher J Sequeira, David J Willis, and Jaime Peraire. Comparing Aerodynamic Models for Numerical Simulation of Dynamics and Control of Aircraft. In *44th AIAA Aerospace Sciences Meeting*, pages 1–20, Reno, Nevada, 2006.

[33] R.R. Lynn. Wing- Rotor Interactions. *Journal of Sound and Vibration*, 4 (3):388–402, 1966.

[34] D.N. Arents. An Assessment of the Hover Performance of the XH-59A Advancing Blade Concept Demonstration Helicopter, 1977.

[35] D. Walsh. High Airspeed Testing of the Sikorsky X2 Technology Demonstrator. In *American Helicopter Society 67th Annual Forum*, Virginia Beach, VA, 2011.

[36] R. Von Mises. *Theory of Flight*. Dover Publications, 1959.

[37] J.D. Anderson. *Fundamentals of Aerodynamics*. McGraw-Hill Book Company, 4th edition, 2007. ISBN 007-125408-0.

[38] H. Yeo and W. Johnson. Optimum Design of a Compound Helicopter. *Journal of Aircraft*, 46(4), 2009. doi: 10.2514/1.40101.

[39] H. Zimmer. The Aerodynamic Calculation of Counter Rotating Coaxial Rotors. In *11th European Rotorcraft Forum*, London, 1985.

[40] J.W. Lim, K.W. McAlister, and W. Johnson. Hover Performance Correlation for Full-Scale and Model-Scale Coaxial Rotors. *Journal of the American Helicopter Society*, 54(3):32005, 2009. doi: 10.4050/JAHS.54.032005.

[41] C.N. Keys. Performance Prediction of Helicopters. In W.Z. Stepniewski, editor, *Rotor-Wing Aerodynamics*. Dover Publications, Inc., 1981.

[42] M. Torres. A Wing on the SA.341 Gazelle Helicopter and its Effects. *Vertica*, 1(1):67–73, 1976.

[43] W. Johnson. *Helicopter Theory*. Dover Publications, Inc., 2nd edition, 1994.

[44] B.L. Stevens and F.L. Lewis. *Aircraft Control and Simulation*. John Wiley and Sons, 2nd edition, 2003. ISBN 0-471-37145-9.

[45] A.R.S. Bramwell. *Helicopter Dynamics*. Edward Arnold, first edition, 1976.

[46] M.V. Cook. *Flight Dynamics Principles*. Elsevier Ltd., 3rd edition, 2013.